ARTICLE IN PRESS

Urban Climate xxx (xxxx) xxx

Contents lists available at ScienceDirect

Urban Climate

journal homepage: www.elsevier.com/locate/uclim

Nature-based solutions in post-industrial sites: Integrated evaluation of atmospheric pollution abatement and carbon uptake in a German city

Martina Ristorini [a,b], Gabriele Guidolotti [b], Gregorio Sgrigna [b], Mais Jafari [c], Dagmar Knappe [c], Vittorio Garfì [a], Chiara Baldacchini [b,d,*], Axel Timpe [e], Carlo Calfapietra [b]

[a] *Department of Bioscience and Territory, University of Molise, 86090 Pesche, IS, Italy*
[b] *Institute of Research on Terrestrial Ecosystems (IRET), National Research Council (CNR), 05010 Porano, TR, Italy*
[c] *Department of Urban Renewal, Kampstraße 47, 44137 Dortmund, Germany*
[d] *Department of Ecological and Biological Sciences (DEB), Università degli Studi della Tuscia, 01100 Viterbo, Italy*
[e] *Institute of Landscape Architecture, RWTH Aachen University, Jakobstraße 2, 52056 Aachen, Germany*

ARTICLE INFO

Keywords:
Nature-based solutions
Ecosystem services
Air quality
Particulate matter
Carbon impact

ABSTRACT

The evaluation of ecosystem services (ESs) provided by Nature-based Solution (NbS) interventions is crucial to assess their efficiency and plan their management. This study focuses on atmospheric pollutants abatement and carbon mitigation potential of tree species (*S. alba* L., *R. pseudoacacia* L., *C. betulus* L., *A. campestre* L., *B. pendula* Roth, *T. cordata* MILL., *S. aucuparia* L.) located in a restored landfill in Dortmund (DE). Leaves from different species were analysed by Scanning Electron Microscopy coupled with Energy-Dispersive X-Ray Spectroscopy, obtaining density, elemental composition and weight of leaf deposited particulate matter (PM) as a function of size fraction and tree species. Experimental $PM_{2.5}$ removal is compared with that obtained by the *i-Tree Eco* model. Modelled removals of O_3, SO_2 and NO_2 are also presented, as well as carbon uptake, from the single tree to the intervention scale. Thus, our study evaluates the provision of ESs for air quality and climate change mitigation by the same NbS intervention, at different scales, and compares experimental and modelling approaches, to highlight limitations and strength points. This represents an important step for the developing of NbS benefits evaluation standards, also providing helpful knowledge for stakeholders and landscape planners in terms of species mitigation efficiency.

1. Introduction

Urban emissions of gaseous pollutants and particulate matter (PM) from vehicular traffic, domestic heating and industrial activities, such as power plants, foundries or refineries, determine frequent exceedances of the air quality standards set by national or international legislations (Rafael et al., 2018; European Environment Agency (EEA), 2016). Combustion processes related to anthropogenic sources are responsible for the emission of gaseous pollutants, such as SO_2 and NO_2. These gases contribute to the acidic

* Corresponding author at: Department of Ecological and Biological Sciences (DEB), Università degli Studi della Tuscia, 01100 Viterbo, Italy.
E-mail address: baldacchini@unitus.it (C. Baldacchini).

https://doi.org/10.1016/j.uclim.2023.101579
Received 12 February 2022; Received in revised form 5 June 2023; Accepted 8 June 2023

deposition, and are precursors of secondary atmospheric PM, with severe consequences on human health and balance of radiative forcings (Singh and Tripathi, 2021; Bishal and Sarkar, 2022). Atmospheric PM is a heterogenous mixture of solid and liquid particles and it is of great risk for human health for accounting for >5% of lung cancer death globally (Ali et al., 2019). In addition, NOx (nitrogen oxides, both NO_2 and N_2O) are known precursors of tropospheric ozone (O_3), which also put at risk human's health and ecosystem functioning (Hui et al., 2023). Increasing urban emissions of gases such as carbon monoxide (CO) and carbon dioxide (CO_2) are also related to climate change, being known as greenhouse gases (GHGs). Atmospheric concentrations of these long-lived GHGs have increased significantly in the last decades (Griffith et al., 2021; Tuckett, 2021), and this has been associated not only to a substantial rise in global average temperatures (Mikhaylov et al., 2020; Lamb et al., 2021) but also to the increased strength and frequency of extreme events (Ebi et al., 2021; Tan et al., 2022).

Therefore, the identification of new and sustainable strategies for the improvement of air quality and climate change mitigation in urban environments is extraordinarily important. Since 2015, the newly developed concept of Nature-based Solutions (NbS) has been introduced by the European Commission (EC) and later defined by the International Union for Conservation of Nature (IUCN) as "actions to protect, sustainably manage, and restore natural or modified ecosystems" (European Commission, 2015; Cohen-Shacham et al., 2016). This concept and its applications address several cross-cutting environmental, social, and economic challenges, in a sustainable and cost-efficient way (Faivre et al., 2017). Indeed, NbS implementation is not only related to the increase of urban resilience, but also to economic and sustainable development, improvement of environmental quality and therefore human health and wellbeing (Carrus et al., 2015; Ruangpan et al., 2020). In this context, the recultivation and afforestation of post-industrial sites is gaining more and more attention from local authorities, stakeholders and scientists (Escobedo et al., 2019; Panno et al., 2017; Song et al., 2019). Among these sites, landfills are a common element of post-industrial landscapes that can be transformed from environmental nuisance into elements of urban green infrastructure, through the NbS concept. Initially located on the periphery of cities, landfills have become more integrated into the urban fabric. This is extremely relevant if the different environmental risks associated to them are considered. For instance, focusing on gaseous emissions, abandoned landfills may release CH_4 and CO_2, due to aerobic and anaerobic decomposition processes. Securing these sites is thus mandatory, and this could be obtained by combining both technical and nature-based solutions, such as the use of sealing layers.

Once safeness is ensured, landfills present a potential for being integrated into the urban green infrastructure as an intervention of NbS, thus being able to provide several ecosystem services (ESs), defined as "benefits that humans derive directly and indirectly from the processes and functions of an ecosystem" (Costanza et al., 1997). Air quality mitigation is one of the most studied ESs in urban contexts (Janhall, 2015; Currie and Bass, 2008), and its provision is linked to the potential of plants to remove gaseous pollutants through stomatal uptake and PM through wet or dry deposition on their foliage (Millennium Ecosystem Assessment (Program), 2005; Nowak et al., 2006;. PM leaf dry deposition is a complex and dynamic mechanism influenced by the chemical-physical characteristics of the particles, by leaves' anatomy and morphology, such as leaf shape, margin and surface structures, and by the meteorological conditions (Sæbø et al., 2012; Wang et al., 2015; Sgrigna et al., 2020; Ristorini et al., 2020a). Greenhouse gases mitigation takes place through atmospheric CO_2 assimilation by photosynthesis and carbon storage (Baro et al., 2014; Myeong et al., 2006). In this case, species-specific characteristics such as tree growth rate, leaf area index, and plant biomass can affect the efficiency of the NbS (Nowak et al., 2002).

The correct assessment of the ESs provided by specific NbSs could allow to evaluate their impact, which is a mandatory step to compare the efficiency of different solutions (Calliari et al., 2019), thus improving the knowledge about NbS design and implementation. However, this task is very complex, and it rarely accounts for the integrative and cross-sectoral approach of the NbS concept, often addressing single ES or challenges (Ordóñez et al., 2019; Farrugia et al., 2015). This is due to complexity and multidimensionality of NbSs, which often address different societal challenges at the same time, sometimes at different spatial scales (Cohen-Shacham et al., 2016). This means that interdisciplinary conceptual and methodological advancements must be considered and taken in account. However, case-studies present in the literature are often focused on single challenge areas or even on single ES (Abson et al., 2014), at specific spatial/temporal scales (Zang et al., 2014). Additionally, and even if more than one ES is assessed, the evaluation of synergies or trade-offs among theme is still a challenge (Seddon et al., 2020; Al Sayah et al., 2021).

To this aim, we focused on an experimental and modelled assessment of the atmospheric pollutants reduction and of the carbon impact of a restored landfill in Dortmund (GE), thus evaluating different ESs provided by the same intervention, at different spatial scale, from the single tree to the whole site. The combination of two methodological approaches, and the comparison of the obtained results, allowed to identify strength points and limitation of the proposed methods. This is extremely important, especially when the modelled approaches are used for the evaluation of ESs, since this often represents a simplification of phenomena, thus being certainly a useful and fast tool, but also requiring consistent validation with experimental data. Furthermore, the single tree approach of our study provided fundamental knowledge on the impact of macroscopic (i.e. tree growth rate, biomass and leaf area) and microscopic (i.e. leaf anatomy or surface roughness) characteristics on the species-specific efficiency in the provision of ESs. Such a species-specific knowledge is crucial to design increasingly efficient NbS in the future, further improving urban life quality and citizen health and wellbeing.

2. Materials and methods

2.1. Study area

The former landfill of Deusen is in the Northwest of the city (51°32′48" N, 7°25′8″ E), in the borough of Huckarde, characterized by the presence of a former mining site and a coking plant, and the district Deusen, from which it takes its name (Fig. 1). Since the beginning of the 20th century, urban waste has been disposed on this site and until its closure in 1992, the Deusen landfill reached a height of 55 m above the surroundings, with 11,000,000 m^3 of waste. Basic recultivation started in 1997, with the step-by-step plantation of about 150,000 trees and shrubs, after drainage and soil cover operations. Within the boundaries of this restored area of about 58 ha, zones with different plant species composition can be identified (indicated by A to F in Fig. 1). As shown in the next Sections, this zonation has been considered for the *i-Tree Eco* modelling of the pollutant removal and carbon impact of the NbS intervention. Biometric details and health status information on the plants located in each zone have been summarized in the Supplementary Materials, S1.

The initial recultivation of the site has been enhanced in stages towards a multifunctional greenspace and it has been further improved within the Horizon 2020 Innovation Action - proGIreg (productive Green Infrastructure for post-industrial urban regeneration) (Jafari et al., 2021). To date, the solutions implemented on the Deusen landfill include different elements as shown in Fig. 2, such as a new path for better access to the site, the plantation of pollinator-friendly vegetation, a mountain bike arena and solar panels.

2.2. *Experimental evaluation of the atmospheric PM abatement*

2.2.1. *Leaf sampling*

The potential of this NbS intervention towards the abatement of airborne PM was assessed through the characterization of leaf deposited particles. Fully-grown leaves were collected from four different tree species: *Acer campestre* L., *Betula pendula* Roth, *Carpinus betulus* L. and *Salix alba* L.. The leaf sampling was carried out on the 18th of September 2019, one month after a precipitation event characterized by a cumulative rainfall of about 12 mm, with a maximum intensity of 6.5 mm/h (occurred in August 15th, 2019; Climate Data Center - Deutscher Wetterdienst - https://cdc.dwd.de/portal/). Indeed, when leaves are sampled to monitor their capability to capture PM, it is important to consider the occurrence of rain events that can remove leaf deposited particles, thus affecting the proper evaluation of PM leaf deposition; generally, the collection of leaves is performed at least one week after a rain event exceeding an intensity of 30 mm/h or 12 mm of cumulative rain (Xu et al., 2017). For each species, six leaves were sampled with telescopic pruning shears, from trees in the East part of the NbS (51°32′51.88"N, 7°25′7.82″E; see Fig. 1) (Sgrigna et al., 2020; Tomašević et al., 2005). Fully grown sun leaves were collected with different cardinal exposures, at 2 m height from ground level. Additionally, and to ensure homogeneity, leaves with a similar position along each branch were selected for SEM/EDX microanalysis. Leaves collected were preserved in paper bags to avoid external contamination and stored in at 4 °C until further analysis.

2.2.2. *SEM/EDX microanalysis of leaf surfaces*

A total of 24 leaves (6 leaves per species) were analysed by a Phenom ProX (PhenomWorld, The Netherlands) scanning electron microscope, equipped with an X-ray analyser (SEM/EDX). Two sections of 0.5 cm^2 (adaxial and abaxial surface) were cut from the same leaf part and mounted on aluminium stubs, by using double coated carbon conductive PELCO Tabs (Ted Pella, Inc.). The two sections were slightly fluxed with compressed air, as recommended by the user manual, and then inserted in the SEM with a charge reduction sample holder, suitable for biological samples. Then, operating in backscattering electron mode, with an incident electron energy of 5 keV, ten micrographs of 150 × 150 μm width (1024 × 1024 pixels resolution) were acquired from each section, for a total of 120 micrographs for each species (60 micrograph for the adaxial and 60 for the abaxial surfaces). Gwyddion v. 2.49 (Nečas and

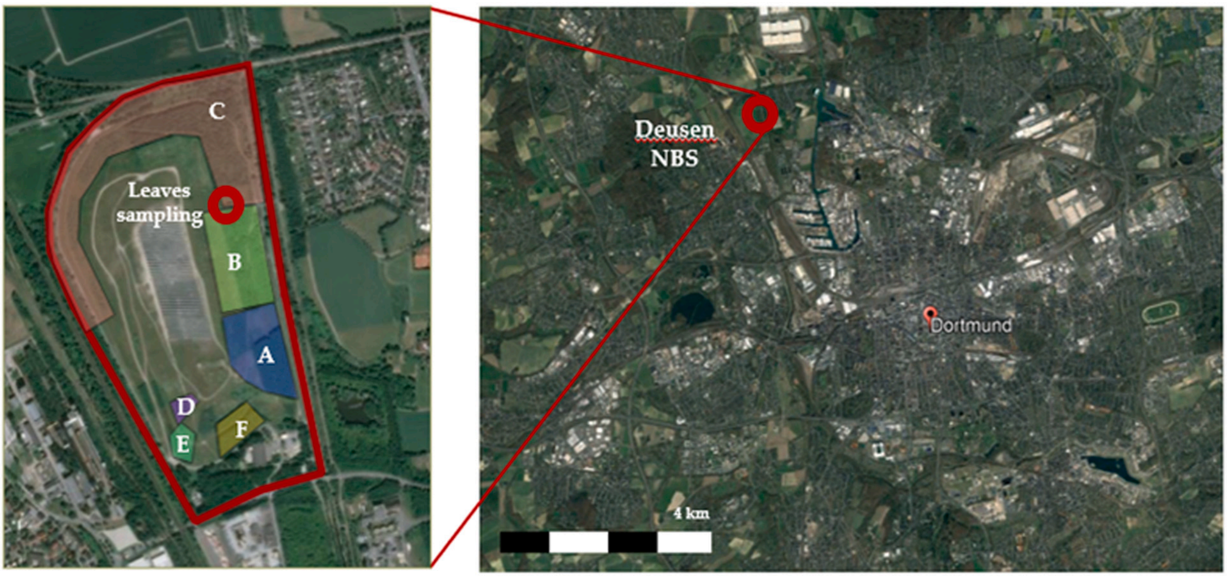

Fig. 1. Deusen previous landfill location and zoomed image, with shown leaves sampling site and areas (A to F) identified for the zonation used for the *i-Tree Eco* modelling, based on the area plant species composition.

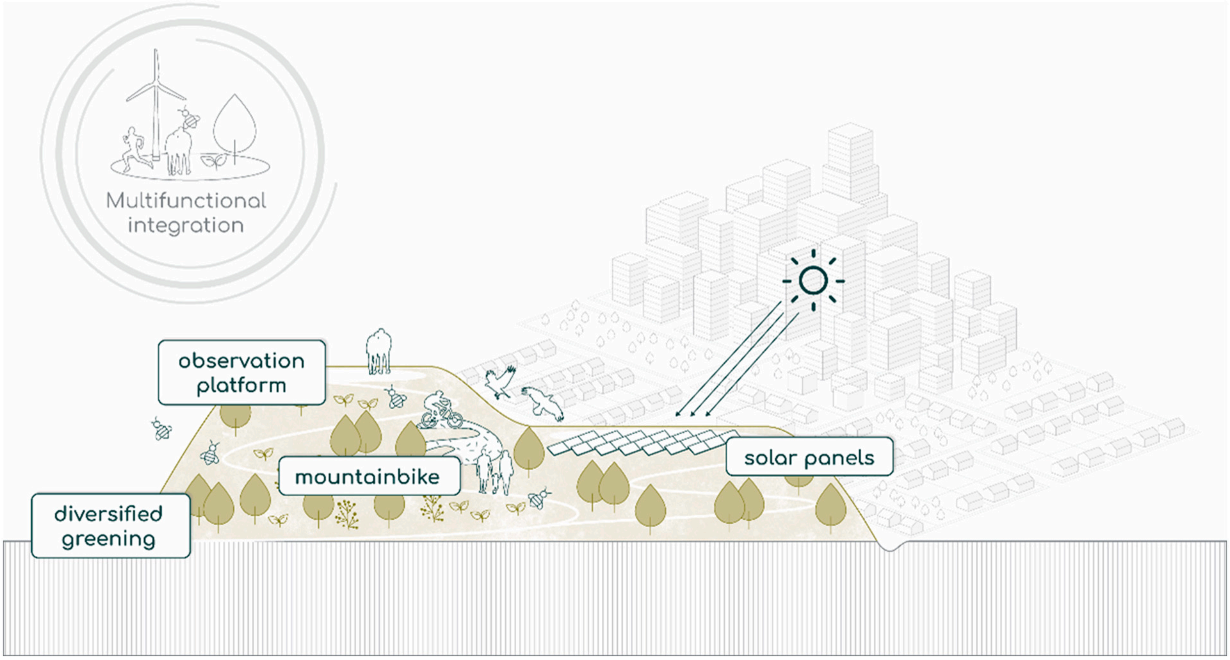

Fig. 2. Different NbSs and other measures combined to make the Deusen landfill a multifunctional green infrastructure: greening with trees and shrubs, accessibility of vistas by steps and walkways, a mountain biking parkours, solar panels and diversified greening for enhancing pollinator friendliness. (For interpretation of the references to colour in this figure legend, the reader is referred to the web version of this article.)

Klapetek, 2012) was used to acquire the number of particles and their equivalent sphere diameter (d_{eq}) (Baldacchini et al., 2017; Merkus, 2009). Therefore, particles density for each species (expressed as the number of particles per unit leaf area in mm^2), was obtained for adaxial (AD) and abaxial (AB) surfaces as a function of size fraction (specifically $PM_{0.2–1}$, particles with aerodynamic diameters from 0.2 μm to 1.0 μm, $PM_{1–2.5}$ with 1.0 μm ≤ a. d. ≤ 2.5 μm, and $PM_{2.5–10}$ with 2.5 μm ≤ a. d. ≤ 10 μm), thus averaging density values obtained from the 60 corresponding micrographs. Standard deviations were also calculated. More detailed information is reported in Baldacchini et al., 2017 (Baldacchini et al., 2017).

Five micrographs of 50 × 50 μm width and same resolution as before were also acquired, with an incident electron energy of 15 keV. From each one, 10 particles were randomly selected for the EDX spectrum acquisition, for a total of 600 particles analysed for each species. Relative percentages of the elemental components, Na, Mg, Al, Si, Cl, K, Ca and Fe,P, S, Ti, Cr, Mn, Ni, Cu an Zn, were acquired. To obtain an estimation of the total PM elemental composition, the weighted volume percentage ($W_{\%x}$) of each element (x) was calculated by multiplying, for each particle (i), the particle volume ($V_i = 4/3\ \pi\ (d_{eqi}/2)^3$) by the element x relative percentage, by summing together the quantities obtained by all the measured particles, and then normalizing the obtained volume by the total measured particle volume (Eq. (1); Baldacchini et al., 2017).

$$W_{\%x} = \frac{\sum_{i=1}^{N} C_{xi} \times V_i}{\sum_{i=1}^{N} V_i} \tag{1}$$

For this part, d_{eq} was obtained through the ImageJ software (Schneider et al., 2012). Then, by averaging these results, mean elemental composition $W_{\%n}$ for each leaf sample (n) and standard deviations, for each size fraction and each species, were obtained. The weight of leaf deposited particles per unit leaf area (μg cm^{-2}) was then calculated taking in account the $W_{\%n}$ of each element, multiplied by the total volume of SEM analysed particles, per each sample, and the corresponding elemental atomic mass per volume (https://www.webelements.com/periodicity/density/), as reported in Baldacchini et al., 2019. These values and standard deviations were calculated for each species and size fraction, thus averaging and combining results from both the AD and the AB surfaces.

2.3. I-Tree Eco model

2.3.1. Biometric, meteorological, and atmospheric pollutants concentrations data

In 2019, data on biometric and health status of trees located in the Deusen NbS were collected. Data such as tree height, diameter of the trunk at the breast height (DBH, approximately 1.3 m from the ground), crown base height and width, percentage of crown missing, crown health and light exposure are required by the *i-Tree Eco* model as input data for estimating parameters such as the leaf area (LA) and the plant dry biomass (Pace et al., 2018), and then modelling the NbS provision of ESs (i-Tree Eco v.6.*0, 2023*). As previously stated, to increase the spatial accuracy in assessing the pollutant removal and carbon impact of the NbS intervention, the landfill area has been divided in the six zones reported in Fig. 1 (A-F), characterized by a different plant species composition, and a significant number of trees for each species was surveyed in each zone, to obtain the average parameters per species per zone. The collected information was then averaged over the total number of trees for each species and within each zone (Supplementary Materials, S1).

The *i-Tree Eco* model also requires hourly meteorological and atmospheric pollutants concentrations data that are retrieved from stations included in the *i-Tree Eco* model database. The closest station to the sampling area have been selected: the Dortmund city airport provided atmospheric concentrations of O_3, NO_2 and $PM_{2.5}$, the station of Recklinghausen (30 km from Dortmund) provided SO_2 concentration, while the nearest station with a complete meteorological data was the station in Maastricht airport (National Center of Environmental Information, NCEI ID: 063800–99,999; 170 km from Dortmund). The most recent available data in the *i-Tree Eco* database were referred to the year 2014.

2.3.2. Modelled removal of O_3, SO_2, NO_2, $PM_{2.5}$ and comparison with experimental $PM_{2.5}$ SEM/EDX results

The *I-Tree Eco* model estimates the removal of O_3, SO_2, NO_2 and $PM_{2.5}$ by the vegetation via deposition or stomatal uptake throughout the year. Pollutant flux (F; expressed in g m^{-2} s^{-1}) of gaseous pollutants is calculated as the product of each pollutant deposition velocity (V_d in m s^{-1}) and their atmospheric concentration (C in g m^{-3}) (Hirabayashi et al., 2012) The V_d for gaseous pollutants (O_3, SO_2, NO_2) are calculated as the inverse sum of the aerodynamic resistance (R_a), quasi-laminar boundary layer resistance (R_b) and canopy resistance (R_c). R_a is calculated using meteorological data, while R_b and R_c are calculated separately for each pollutant (Pace et al., 2018). $PM_{2.5}$ flux and V_d calculations are mainly affected by wind speed and LA (Nowak et al., 2013). Each modelled pollutant flux is multiplied for the modelled LA, to achieve the mass removed through dry deposition ($PM_{2.5}$) or stomatal uptake (gaseous pollutants) by the vegetation. The removed mass of each pollutant in one year, by single trees of each species and by the total number of trees located in this NbS intervention were accurately estimated. For those species that have been reported to have trees with different biometric characteristics and/or health status, results were summed together (Supplementary Materials, S1), obtaining a single value for each species. Since we are interested in comparing the potential removal of the different zones by taking into account only their plant species composition, while these zones are characterized also by different areas, the removal values of each zone and of the total NbS intervention have been normalized by their areas in hectares, obtaining the kg of pollutants removed throughout the year per unit area (kg ha^{-1} $year^{-1}$). For each modelled value obtained (single tree, zone upscale, total NbS) the associated uncertainty was calculated (Taylor, 1982). Specifically, percentage uncertainties were calculated as the square root of the sum of squared percentage uncertainties for each single factor considered in the modelling and in the upscale. The single factor uncertainties were estimated by the experimental data dispersion or by the standard deviation, depending on the data structure.

Finally, modelled removal results of $PM_{2.5}$ were compared with the experimental ones obtained from SEM/EDX. The comparison concerned only the species analysed by SEM/EDX. Species-specific mass concentrations of $PM_{2.5}$ obtained through the SEM/EDX procedure were multiplied by the LA (in cm^2) modelled by *i-Tree Eco* for single trees of *Acer campestre* L., *Betula pendula* Roth, *Carpinus betulus* L. and *Salix alba* L.. These latter results were considered representative of about one-month PM leaf dry deposition, due to the occurrence of last intense precipitation event in Dortmund city (15th of August 2019) before the leaf sampling date (Climate Data Center - Deutscher Wetterdienst - https://cdc.dwd.de/portal/). To finalize the comparison, the yearly *i-Tree Eco* $PM_{2.5}$ outputs were normalized accounting a leafy period length of eight months.

2.3.3. Carbon storage and carbon gross sequestration

Carbon storage describes the difference between the amount of carbon stored in the plant dry biomass via total photosynthesis, and the one lost by respiration, while carbon gross sequestration is the yearly rate of carbon removal from the atmosphere (Martin et al., 2012). The above-ground plant dry biomass is calculated through DBH and allometric equations. To estimate the total biomass (above and below ground), a root to shoot ratio of 0.26 was applied. Since the allometric equations are diameter-based and developed for closed canopies, biomass was reduced by a factor of 0.8, to account the influence of urban open-growth conditions on the above ground biomass (Pace et al., 2018).

The modelled carbon gross sequestration is calculated thus considering a standard diameter growth of tree which accounts of the tree light exposure and the number of frost days in the studied years (Nowak and Crane, 2002; Nowak, 1994). Specifically, for open-grown trees with a Crown Light Exposure (CLE) ranging from 4 to 5, the Standard diameter Growth (SG) is calculated as SG 0.83 cm/ year × (number of frost-free days/153); for park trees (CLE = 2–3) and forest trees (CLE = 0–1), SG is calculated by dividing the corresponding value for open-grown trees by 1.78 and by 2.29, respectively.

As for the removal of atmospheric pollutants, the individual tree results for carbon storage and gross sequestration (expressed in kg and kg $year^{-1}$, respectively) were then upscaled for the total number of trees for each species. Results of each zone and of the total NbS were furtherly normalized by their areas in hectares, obtaining the kg ha^{-1} of carbon stored/sequestrated in one year. Also, for these parameters, uncertainties were calculated as reported in Section 2.3.2.

3. Results and discussion

3.1. PM abatement estimated by SEM/EDX microanalysis

3.1.1. Density of leaf deposited PM

The averaged species-specific particle densities (number of particles per unit leaf area in mm^2), with standard deviations were obtained from the SEM images of the adaxial (AD) and abaxial (AB) leaf surfaces (Supplementary Materials, S2), for three size fractions: ultrafine ($PM_{0.2–1}$), fine ($PM_{1–2.5}$) and coarse ($PM_{2.5–10}$) PM (Supplementary Materials, S3). The mean particle density on the AB surfaces of the selected trees ($1.96 \pm 0.23 * 10^4$ particles mm^{-2}) was about the 70% of that on the AD surfaces ($2.90 \pm 0.37 * 10^4$ particles mm^{-2}), with density values that are consistent with those previously reported for leaf-deposited PM in urban context (Weerakkody et al., 2017; Baldacchini et al., 2017; Baldacchini et al., 2019). The observed difference between particle densities on the AD and AB leaf surfaces is a direct consequence of their orientation and, therefore, different interaction with wind turbulence (Baldacchini et al., 2017; Ottele et al., 2010; Shi et al., 2008). If the total $PM_{0.2–10}$ leaf deposited particles were considered, no statistically significant differences were detected among the four species. Concerning the size fractions, the $PM_{0.2–1}$ was the most abundant one in terms of particles density, ranging from 90% to 93.1% for AD surfaces (respectively for *A. campestre* and *S. alba*) and from 91.7% to 93.6% for AB surfaces (respectively for *B. pendula* and *S. alba*). The $PM_{1–2.5}$ was represented by percentages ranging from 6.3% (*S. alba*) to 8.8% (*A. campestre*) in the AD surfaces, while for the AB ones, these percentages ranged from 6.0% (*A. campestre*) to 7.5%

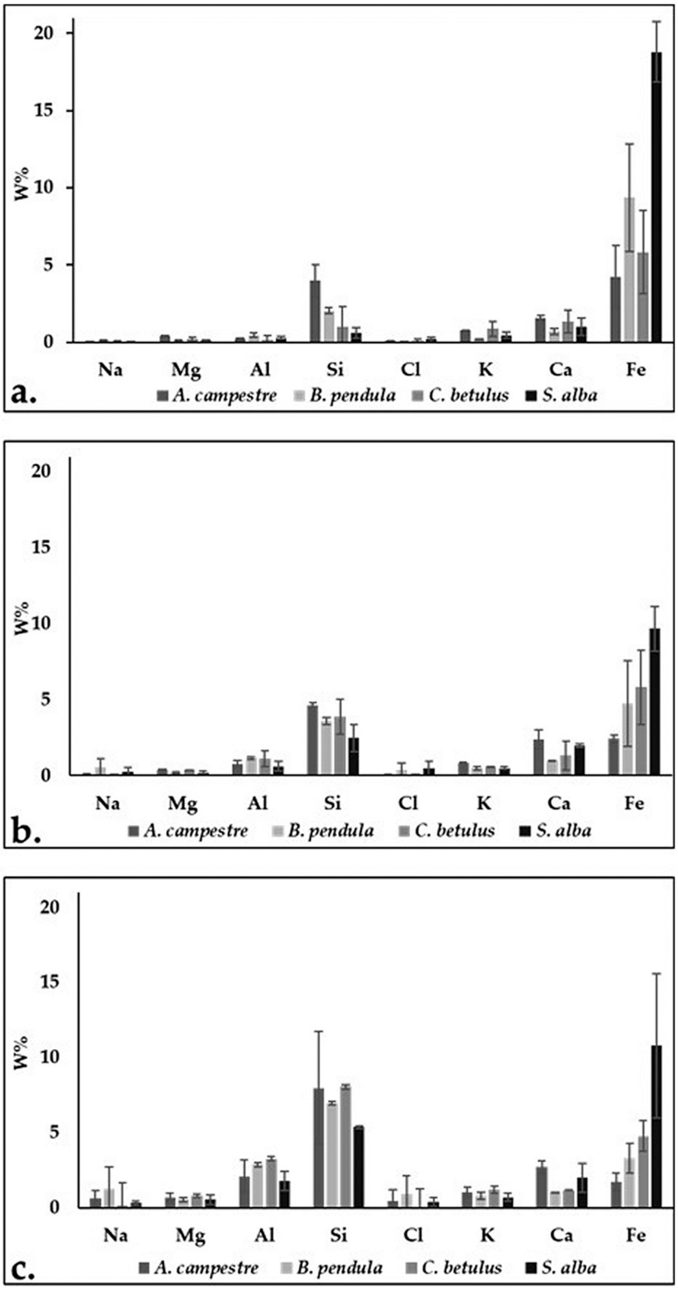

Fig. 3. Relative elemental composition and standard deviations, as estimated by the $W_{\%}$ obtained from the SEM/ EDX analysis, for the 3 PM size fractions (a. $PM_{0.2–1}$; b. $PM_{1–2.5}$; c. $PM_{2.5–10}$), for all the species.

(*B. pendula*). Finally, the AD coarse particles ($PM_{2.5–10}$) ranged from 0.5% (*B. pendula*) to 1.1% (*A. campestre*), comparable to the range of AB ones (0.5% - 0.8%). However, the mean density values per size fraction and per species are not significantly different, with the exception of the high $PM_{2.5–10}$ density observed on the AD surface of *A. campestre* (400 ± 50 particles mm^{-2}). The high accumulation of coarse particles in *A. campestre* leaves was also described in Dzierżanowski et al., 2011, which reported a high accumulation of $PM_{2.5–10}$ particles both in superficial parts of leaves and in waxes.

3.1.2. Elemental composition of leaf deposited PM

For all the considered size fractions and species, sodium (Na), magnesium (Mg), aluminium (Al), chlorine (Cl), potassium (K), calcium (Ca) and iron (Fe) were the major components of leaf deposited particles, being characterized by a $W_{\%}$ higher than 1%. Some general trends could be described for the size distribution of these major elemental components. All the accounted tree species were characterized by a decrease of $W_{\%}$ for elements such as Na, Cl, Mg, Al, and Si, from coarse particles ($PM_{2.5–10}$) to ultrafine ones ($PM_{0.2–1}$) (Fig. 3). These elements are known to be typical crustal components and for this reason often used as tracers for natural soil resuspension (Abhijith and Kumar, 2020). In our study, the size distribution detected for these elements (higher $W_{\%}$ in the coarse PM) confirmed the origin of these particles and also the role of these elements as selective tracers for this kind of natural emission source (soil resuspension) (Amato et al., 2009). On the other hand, Fe, which is often associated to anthropogenic emission sources, such as vehicular traffic and industrial activities (Massimi et al., 2020; Ristorini et al., 2020b), was mostly abundant in the ultrafine particles fraction (Fig. 3), as well as trace elements, i.e. those element with W% lower than 1%, such as titanium (Ti), chromium (Cr) and manganese (Mn) (data not shown). Also in this case, the size distribution of these elements (higher $W_{\%}$ in the ultrafine PM) may confirm the origin of these particles, which are characterized by a smaller aerodynamic diameter, thus connecting their prevalent emission to combustion related processes (Massimi et al., 2019; Davila et al., 2006).

Interestingly, and in contrast to what was detected for the particle density, differences between the elemental composition of PM were observed across the four tree species. *S. alba* leaves had the highest number of iron-containing particles, in both $PM_{2.5–10}$ and $PM_{0.2–1}$ fractions, with a Fe $W_{\%}$ of 10.8% and 18.8%, respectively. These were the highest percentages measured for all the species and for all the fractions (Fig. 3). *S. alba* confirmed this trend in $PM_{1–2.5}$ fraction also for others trace elements, such as chromium (Cr, $W_{\%}$ = 0.19%) and titanium (Ti, $W_{\%}$ = 0.26%), thus revealing a specific affinity for the removal of heavy metal from the atmosphere. On the other hand, *A. campestre* leaves were characterized by $PM_{0.2–1}$ with a significantly higher concentrations of Si ($W_{\%}$ = 3.99%) and Ca ($W_{\%}$ = 1.58%), thus indicating a low affinity of this species towards heavy metal containing particles also in the ultrafine fraction, where these latter elements are generally more abundant. No significant differences were found between the $W_{\%}$ of the other elemental components, for all the size fractions.

3.1.3. Mass concentration of leaf deposited PM

The mass of removed PM per unit leaf area (μg cm^{-2}), for each species and size fraction, is shown in Fig. 4. *S. alba* and *A. campestre* had the highest total $PM_{0.2–10}$ mass accumulated on their leaves, corresponding to 3.84 ± 0.36 μg cm^{-2} and 3.23 ± 0.23 μg cm^{-2} respectively, while *C. betulus* leaves were the less efficient, with a mean load of 1.92 ± 0.14 μg cm^{-2}. The same trend was obtained for the coarse PM size fraction ($PM_{2.5–10}$), which is known to mainly drive the mass load of $PM_{0.2–10}$ (Cai et al., 2017). Instead, for both $PM_{1.2,5}$ and $PM_{0.2–1}$ fractions, only *S. alba* leaves showed a particle load that was significantly higher than the others (0.68 ± 0.11 μg cm^{-2} for $PM_{0.2–1}$ and 1.07 ± 0.13 μg cm^{-2} for the $PM_{1.2,5}$).

Overall, *S. alba* resulted to be the species with the highest mass of leaf deposited particles, for all the studied size fractions. Particles density on leaves was comparable among the species, as discussed, but *S. alba* showed the highest affinity towards heavy metal containing particles, which are characterized by a higher elemental atomic mass and, therefore, weight mass (Section 3.1.2). This results in the higher PM load observed on *S. alba* leaves, and it could be used as a valid proxy for its potential removal affinity towards airborne PM. Instead, the high PM mass concentrations detected for total PM ($PM_{0.2–10}$) and coarse fraction ($PM_{2.5–10}$) in *A. campestre*

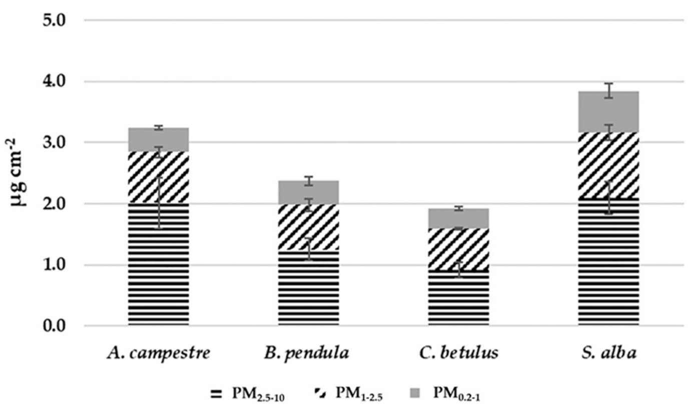

Fig. 4. PM mass concentration on leaves (μg cm^{-2}), as obtained from SEM/EDX, through the combination of PM density and elemental composition results, as averaged values over the six leaves per each species. Standard deviations are given for each size fraction and each species.

leaves can be explained by the high particle densities detected on its leaf samples in the coarse size fraction (Section 3.1.1). *C. betulus* and *B. pendula* were then the species with the lowest accumulated PM loads, for every considered size fraction. For *C. betulus*, in particular, our results may highlight the impact of species-specific anatomical characteristics on PM capturing capabilities, since its leaves are known to be characterized by smooth surfaces, which may negatively interfere with their ability to withhold deposited particles (He et al., 2020; Przybysz et al., 2019; Sgrigna et al., 2020). However, in our study, inter-specific variability was lower than expected, and often not significant, and this may be explained by taking in account the proximity of the sampled plants in a densely forested area, which could have determined a quite homogeneous conditions of leaf exposure to airborne PM.

3.2. *I-Tree Eco model evaluation of atmospheric pollutant removal (O_3, SO_2, NO_2 and $PM_{2.5}$)*

Modelled results relative to the removal of O_3, SO_2, NO_2 and $PM_{2.5}$ by single trees showed a high inter-specific variability (Table 1). For $PM_{2.5}$, the highest removal efficiency was observed for *S. alba*, followed by *R. pseudoacacia*, *C. betulus* and *A. campestre*, while *S. aucuparia, B. pendula* and *T. cordata* were the less efficient species. Yearly removal of $PM_{2.5}$ ranged from a minimum of 0.10 ± 0.02 g, detected for single trees of *S. aucuparia*, to a maximum of 11.8 ± 2.1 g, for *S. alba* (Table 1). Similar trend could be observed also for O_3, SO_2 and NO_2, confirming *S. alba* as the species with the highest removal modelled values, which are up to 162.8 ± 27.4 g for O_3, 93.1 ± 27.4 g for NO_2 and 8.6 ± 1.5 g of SO_2 (Table 1). Biometric and health status data, which are required by the model to calculate the LA associated to each plant, determine a higher or lower removal of atmospheric pollutants, thus being the main factors affecting the modelling of this ESs. Indeed, plants with the highest biometric/health status values (Supplementary Materials S1) are also those with the highest modelled values of LA and, therefore, those for which the highest removal of atmospheric pollutants is obtained. The described approach may be considered to deduce which species are the more adapted to survive and grow in urban environments, thus providing relevant information for the preliminary stages of NbS design and for the selection of the most efficient tree species.

Zone E, characterized by the co-presence of two different types of *B. pendula* trees, which differ for the percentage of crown missing (20% or 40%) and for their crown light exposure (3 or 4), was the most effective towards the removal of $PM_{2.5}$, followed by Zone A and B (Table 1). Likewise, Zone E was confirmed as the one with the highest annual removal of gaseous pollutants that was 189.8 ± 38.0 kg ha^{-1}, 109.2 ± 21.2 kg ha^{-1}, 9.7 ± 2.0 kg ha^{-1} for O_3, NO_2 and SO_2, respectively (Table 1). Conversely, Zone D, characterized by two *S. aucuparia* trees having different percentage of crown missing (20% or 40%) and crown light exposure (1 or 4), was the least efficient one (6.8 ± 1.3 kg ha^{-1} of O_3, 3.9 ± 0.7 kg ha^{-1} of NO_2 and 0.4 ± 0.1 kg ha^{-1} of SO_2 removed each year). In Zone E, the high tree density overcame the limited removal of its main species (*B. pendula*), while the high removal values obtained for zone A and B, may be due to the presence of highly removing species, i.e. *R. pseudoacacia* (zone A) and *S. alba* (zone B). The sum of the various zones provides the pollution removal by the total NbS: 46.4 ± 10.7 kg ha^{-1} of O_3, 26.5 ± 6.0 kg ha^{-1} of NO_2, 2.4 ± 0.6 kg ha^{-1} of SO_2 and 3.4 ± 0.8 kg ha^{-1} of $PM_{2.5}$, for a total of 78.7 ± 15.7 kg ha^{-1} of pollutants removed (Table 1).

As previously described (Section 2.3.2), the *i-Tree Eco* modelling of air pollutant removal is strongly affected by the field data collection used to calculate the LA of each single tree. The plants with a highest modelled LAs have also the highest removal potentials. Indeed, when trees were surveyed in this NbS, *S. alba* trees were the most healthful and grown ones, thus showing the highest values for each biometric or health status category, such as DBH, crown width, health, and light exposure, and on the other hand, lower percentages of crown missing (Supplementary Materials S1). On the contrary, *S. aucuparia* trees significantly differed from the others, having the lowest recorded biometric values. Also, trees from *B. pendula* and *T. cordata* species were characterized by low crown width (1.5 m), low light exposure and a high percentage of crown missing (up to 50%), thus resulting in a low removal efficiency. It is important to underline that the species-specific affinity towards the removal of atmospheric pollutants, described in this Section, as

Table 1
I-Tree Eco modelled potential removal of atmospheric pollutants O_3, SO_2, NO_2 and $PM_{2.5}$. Single tree results for each species (g of pollutant removed $year^{-1}$) together with zone and total NbS results (kg of pollutant removed ha^{-1} $year^{-1}$) are presented. The uncertainties associated to each value are also presented.

Grams per single tree per year	$PM_{2.5}$	O_3	NO_2	SO_2
S. alba L.	11.8 ± 2.1	162.8 ± 27.4	93.1 ± 15.0	8.6 ± 1.5
R. pseudoacacia L.	5.5 ± 1.0	76.5 ± 12.9	43.7 ± 7.1	4.0 ± 0.7
C. betulus L.	4.5 ± 0.8	61.6 ± 10.4	35.2 ± 5.7	3.3 ± 0.6
A. campestre L.	2.5 ± 0.4	34.5 ± 5.8	19.7 ± 3.2	1.8 ± 0.3
B. pendula Roth	1.2 ± 0.2	16.3 ± 2.7	9.3 ± 1.5	0.9 ± 0.2
T. cordata MILL.	0.6 ± 0.1	9.2 ± 1.5	5.2 ± 0.8	0.4 ± 0.1
S. aucuparia L.	0.10 ± 0.02	1.4 ± 0.2	0.8 ± 0.1	0.10 ± 0.02

Kilograms per hectare per year	$PM_{2.5}$	O_3	NO_2	SO_2
Zone A	9.6 ± 2.0	132 ± 26	75.6 ± 14.7	7.0 ± 1.4
Zone B	3.4 ± 0.7	47.9 ± 9.6	27.4 ± 5.3	2.3 ± 0.5
Zone C	1.7 ± 0.3	22.7 ± 4.5	13.0 ± 2.5	1.2 ± 0.2
Zone D	0.4 ± 0.1	6.8 ± 1.3	3.9 ± 0.7	0.4 ± 0.1
Zone E	13.7 ± 2.9	190 ± 38	109 ± 21	9.7 ± 2.0
Zone F	2.9 ± 0.6	40.2 ± 7.6	23.0 ± 4.2	2.1 ± 0.4
Total NbS	3.4 ± 0.8	46.4 ± 10.7	26.5 ± 6.0	2.4 ± 0.6

well the carbon impact described later in this study, may change over time, if the different growth rates of the trees species are considered.

The *i-Tree Eco* model has been often applied to assess air pollution mitigation at the city level, while very few examples of NbS modelling can be found. In our case, the identification of the restored landfill of Deusen as study area, allowed the evaluation of this regulating ES at this smaller scale (NbS one), thus providing a quantitative estimation of the provision of these air quality related benefits by the vegetation. Even if the use of no-local meteorological data may have affected the annual O_3, NO_2 and SO_2 removal estimation obtained for the Deusen NbS, these resulted to be within the ranges reported in other studies (Nowak et al., 2006. This is an important result considering the high number of factors affecting air pollution removal such as tree species, plants health status, meteorological conditions and finally pollutants atmospheric concentrations (Guidolotti et al., 2016).

3.3. Intercomparison between SEM/EDX and i-Tree Eco $PM_{2.5}$ removal results

The scaled up values of the amount of $PM_{2.5}$ removed in one month by a single tree per each tree species were estimated from the *i-Tree Eco* modelled values and from the loads obtained by SEM/EDX, and then compared in Fig. 5. Although the general trend showed by the two techniques was similar, the modelled values were always lower than those assessed by SEM/EDX, especially in the case of *S. alba*.

This could be explained by the presence of some gross approximations in the *i-Tree Eco* model. Firstly, the modelling of the atmospheric pollutant removal in the model is based on a V_d that is dependent on the pollutant type and not on the tree species, thus neglecting that species-specific traits and their impact on PM leaf deposition such as leaf morphological traits (Sæbø et al., 2012; Sgrigna et al., 2020; Dzierżanowski et al., 2011) and structure of the vegetation as a function of height and density (Abhijith and Kumar, 2020). This may be connected to the larger underestimation detected especially for single trees of *S. alba*, which among the other species is characterized by peculiar characteristic both in terms of crown structure and morphology (high density of leaves) and in terms of leaf anatomy (presence of trichomes). Then, the model assumes that hourly meteorological and atmospheric pollutants concentration data are homogeneous over a region (Cabaraban et al., 2013), this implying that only one station can be sourced for each type of data, within the model database. This further approximation can be certainly considered as relevant in negatively affecting the modelling of the air quality improvement by urban trees, thus often determining a model underestimation (Riondato et al., 2020). A better parameterization of the *i-Tree Eco* model, accounting for species-specific deposition velocities, together with a wider set of usable meteorological/pollution stations may guarantee a more accurate estimation and a better validation with experimental data (Pace et al., 2021).

3.4. I-Tree Eco model evaluation of carbon storage and gross sequestration

The Deusen NbS showed a total dry biomass of 352.6 ± 88.9 tons ha^{-1} and an annual carbon gross sequestration of 12.8 ± 2.4 tons ha^{-1} year^{-1}. Carbon storage of single trees ranged from a minimum of 17.7 ± 4.5 kg for *S. aucuparia* to a maximum of 4844.2 ± 1223.6 kg for *S. alba* (Table 2). This latter species, with 3500 trees on a total of 63,000 trees, accounted for 82% of the total NbS carbon storage, followed by relatively small percentages of *B. pendula* (7.5%) and *R. pseudoacacia* (4.6%). Also in this case, the results were strongly dependent on the field data collection, in particular DBH, as described in Section 2.3.3. Indeed, the higher values obtained for *S. alba* trees corresponded to the highest DBH values among all the studied species.

The carbon gross sequestration (expressed as kg year^{-1}) was directly influenced by the crown light exposure (Supplementary Materials, S1). The *i-Tree Eco* model assigns to this parameter a high influence on trees growth and therefore their ability to sequestrate

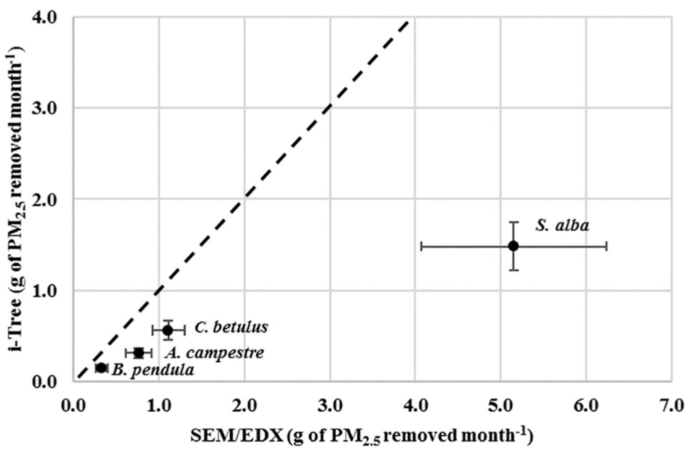

Fig. 5. Kg of $PM_{2.5}$ removed in one month by single trees of the four considered species (*A. campestre*, *B. pendula*, *C. betulus* and *S. alba*). Standard deviations calculated for SEM/EDX experimental mass concentrations and uncertainties calculated for the *i-Tree Eco* modelling results are also reported. The dashed line represents the 1:1.

atmospheric carbon. Indeed, this was connected to the 110.3 ± 20.4 kg year^{-1} detected also in this case, for *S. alba,* followed by *B. pendula* (11.6 ± 2.1 Kg year^{-1}), *C. betulus* (7.4 ± 1.4 kg year^{-1}) and *R. pseudoacacia* (6.0 ± 1.1 kg year $^{-1}$) (Table 2). For all these species, higher light crown exposures were reported, with values ranging between 4 and 4.5. As in the case of air pollutant removal, the species-specific affinity towards these carbon related ESs, which are directly influenced by the tree health and grown status, may indirectly provide information on the adaptability of single species to this specific urban context. This is true since the most grown plants are expected to be also the ones with higher adaptability to the highly stressful living conditions of these environments. The highest tree density detected in the NbS and the massive presence of *B. pendula* trees in the Zone E, determined higher values per unit area for both carbon storage and carbon sequestration (1277.4 ± 322.1 tons ha^{-1} and 130.2 ± 24.0 tons ha^{-1} year^{-1}, respectively). Also Zone B, composed by 5500 trees distributed between *A. campestre* and *S. alba*, resulted in high carbon storage (984.7 ± 248.5 tons ha^{-1}) and sequestration (20.0 ± 3.7 tons ha^{-1} year^{-1}) (Table 2).

It is important to underline that when the carbon mitigation potential of urban green areas is investigated, it should be also needed to compare these data to urban carbon emissions data, to evaluate their real impact. The Global Covenant of Mayors for Climate and Energy, which gathers a multitude of local governments engaged in the reduction of GHGs emissions, reported for Dortmund city a baseline (referred to the year 2008) of GHGs emission of about 9 million tons (https://www.globalcovenantofmayors.org/). The Deusen NbS, that is only one of the several green areas of the city of Dortmund covering about the 0.21% of the city, was able to store in its dry biomass the 0.22% of the carbon emitted by the city. Interestingly, this percentage results to be in agreement with those reported for other green areas of different European cities (Baró et al., 2015). Taking into account the previously described results, it is worth noticing that if this urban forest was exclusively composed by *S. alba* trees, the ones with the higher adaptability, it would be able to store up to 3.4% of carbon emitted, with about 305 thousand tons stored in its biomass. This underlines the importance of a proper selection of species, based on an accurate quantification of their affinity towards the provision of ESs and their adaptability, in the design of highly efficient NbS. For a proper assessment of the climate change mitigation potential of urban green areas, it would be necessary to consider the whole carbon balance (Kabisch et al., 2017; Nicese et al., 2021) thus accounting also for all GHG emissions connected to the NbS implementation and maintenance (e.g soil preparation, pruning, etc), decomposition rate of removed plants and also the role of soil as natural carbon sink and source.

4. Conclusions

This study is focused on the evaluation of the atmospheric pollutants removal and the carbon sequestration of an NbS intervention on a former landfill in Dortmund (DE), while assessing the efficiency in ES provision of the different tree species present in the study site. Firstly, the PM removal, per size fraction, has been experimentally obtained, from the single leaf to the whole tree scale. *S. alba* resulted as the most efficient species towards the PM removal via leaf deposition, in every size fraction considered, being able to remove a maximum of 3.8 ± 0.4 μg cm^{-2} of leaf unit area of $PM_{0.2–10}$., likely due to its high affinity towards heavy metal composed PM particles. The experimental PM removals have been compared with the output obtained by *i-Tree Eco* model, with the confirmation of the species-specific trend, despite the modelled data were systematically underestimated. This shows the limitation of modelling approaches, when they include strong approximations, such as the lack of species-specific parametrization of the PM deposition velocity in *i-tree Eco*, and thus the need of experimental validations of modelling approaches, due to their exponentially growing application in the estimation of ESs' provision. However, despite these limitations, the modelling outputs we obtained confirmed their usefulness, for instance by demonstrating how plant morphology and adaptability can compensate for low PM removal efficiency at the leaf level, as in the case of *B. pendula*. Moreover, modelled carbon impact of Deusen trees gave important information about the relation among carbon storage and gross sequestration and plant health status, which is directly connected with the amount of dry biomass and the trees rate of growth. Among the tree species, *S. alba* emerged as that having the major impact for all the ESs, both in air pollutant removal and in carbon mitigation being the ones with highest values of biometric and health status, due to the good adaptability of this species in the study area. Thus, as a further result, our study underlines how some of the main advantages that may be connected to the implementation of NbS such as the afforestation of post-industrial sites, are largely dependent on the species selection and related plant resilience, which will be more and more important in view of future climatic *scenarios*.

Funding

The research leading to these results has received funding from the European Union's Horizon 2020 Innovation Action Program under Grant Agreement no. 776528. The sole responsibility for the content lies with the proGIreg project and in no way reflects the views of the European Union.

CRediT authorship contribution statement

Martina Ristorini: Methodology, Formal analysis, Investigation, Writing – original draft, Visualization. **Gabriele Guidolotti:** Methodology, Formal analysis, Investigation, Writing – review & editing. **Gregorio Sgrigna:** Formal analysis, Investigation. **Mais Jafari:** Resources. **Dagmar Knappe:** Resources. **Vittorio Garfì:** Writing – review & editing. **Chiara Baldacchini:** Conceptualization, Methodology, Formal analysis, Writing – review & editing, Visualization. **Axel Timpe:** Resources, Writing – review & editing, Visualization, Project administration, Funding acquisition. **Carlo Calfapietra:** Writing – review & editing, Supervision, Project administration, Funding acquisition.

Table 2
I-Tree Eco modelled carbon storage and sequestration. Single tree results (respectively expressed in kg and in kg year^{-1}) together with zone and total NbS results (tons ha^{-1} and tons ha^{-1} year^{-1}) are presented with calculated uncertainties.

Kilograms per single tree	C storage	C sequestration per year
Salix alba L.	4844 ± 1224	110 ± 20
Betula pendula Roth	80.7 ± 20.3	11.6 ± 2.1
Robinia pseudoacacia L.	62.0 ± 15.6	6.0 ± 1.1
Carpinus betulus L.	49.3 ± 12.4	7.4 ± 1.4
Acer campestre L.	45.3 ± 11.4	3.5 ± 0.6
Tilia cordata L.	39.0 ± 9.8	3.5 ± 0.6
Sorbus aucuparia L.	17.7 ± 4.5	4.2 ± 0.8

Tons per hectare	C storage	C sequestration per year
Total NbS	353 ± 89	12.8 ± 2.4
Zone A	105 ± 26	7.6 ± 1.4
Zone B	985 ± 248	20.0 ± 3.7
Zone C	225 ± 57	8.2 ± 1.5
Zone D	84 ± 21	13.8 ± 2.6
Zone E	1277 ± 322	130 ± 24
Zone F	218 ± 55	19.6 ± 3.6

Declaration of Competing Interest

The authors declare no conflict of interest. The funders had no role in the design of the study; in the collection, analyses, or interpretation of data; in the writing of the manuscript, or in the decision to publish the results.

Data availability

Data will be made available on request.

Acknowledgments

The authors thank Arianna Calabresi for preliminary measurements and Dania Valli for supporting data acquisition.

Appendix A. Supplementary data

Supplementary data to this article can be found online at https://doi.org/10.1016/j.uclim.2023.101579.

References

Abhijith, K.V., Kumar, P., 2020. Quantifying particulate matter reduction and their deposition on the leaves of green infrastructure. Environ. Pollut. https://doi.org/10.1016/j.envpol.2020.114884.

Abson, D.J., von Wehrden, H., Baumgärtner, S., Fischer, J., Hanspach, J., Härdtle, W., Heinrichs, H., Klein, A.M., Lang, D.J., Martens, P., Walmsley, D., 2014. Ecosystem services as a boundary object for sustainability. Ecol. Econ. 103, 29–37. ISSN 0921–8009. https://doi.org/10.1016/j.ecolecon.2014.04.012. ISSN 0921–8009.

Al Sayah, M., Versini, P.A., Schertzer, D., 2021. Nature Based Solutions: Reporting and analyzing insights from Europe, EGU General Assembly 2021, online, 19–30 Apr 2021, EGU21–8902. https://doi.org/10.5194/egusphere-egu21-8902.

Ali, M.U., Liu, G., Yousaf, B., Ullah, H., Abbas, Q., Munir, M.A.M., 2019. A systematic review on global pollution status of particulate matter-associated potential toxic elements and health perspectives in urban environment. Environ. Geochem. Health 41, 1131–1162. https://doi.org/10.1007/s10653-018-0203-z.

Amato, F., Pandolfi, M., Viana, M., Querol, X., Alastuey, A., Moreno, T., 2009. Spatial and chemical patterns of PM10 in road dust deposited in urban environment. Atmos. Environ. 43 (9), 1650–1659. https://doi.org/10.1016/j.atmosenv.2008.12.009.

Baldacchini, C., Castanheiro, A., Maghakyan, N., Sgrigna, G., Verhelst, J., Alonso, R., Amorim, J.H., Bellan, P., Bojović, D.D., Breuste, J., et al., 2017. How does the amount and composition of PM deposited on *Platanus acerifolia* leaves change across different cities in Europe? Environ. Sci. Technol. 51, 1147–1156. https://doi.org/10.1021/acs.est.6b04052.

Baldacchini, C., Sgrigna, G., Clarke, W., Tallis, M., Calfapietra, C., 2019. An ultra-spatially resolved method to quali-quantitative monitor particulate matter in urban environment. Environ. Sci. Pollut. Res. 26, 18719–18729. https://doi.org/10.1007/s11356-019-05160-8.

Baro, F., Chaparro, L., Gomez-Baggethun, E., Langemeyer, J., Nowak, D.J., Terradas, J., 2014. Contribution of ecosystem services to air quality and climate change mitigation policies: the case of urban forests in Barcelona, Spain. AMBIO 43, 466–479. https://doi.org/10.1007/s13280-014-0507-x.

Baró, F., Haase, D., Gómez-Baggethun, E., Frantzeskaki, N., 2015. Mismatches between ecosystem services supply and demand in urban areas: a quantitative assessment in five European cities. Ecol. Indic. 55, 146–158.

Bishal, P., Sarkar, A., 2022. Acid deposition: anthropogenic causes, destructive effects and probable remedies. Int. J. Chem. Environ. Sci. 4.1 (2022), 30–37. https://doi.org/10.15864/ijcaes.4103.

Cabaraban, M.T.I., Kroll, C.N., Hirabayashi, S., Nowak, D.J., 2013. Modeling of air pollutant removal by dry deposition to urban trees using a WRF/CMAQ/i-Tree Eco coupled system. Environ. Pollut. 176, 123–133. https://doi.org/10.1016/j.envpol.2013.01.006.

Cai, M., Xin, Z., Yu, X., 2017. Spatio-temporal variations in PM leaf deposition: a meta-analysis. Environ. Pollut. 231 (Pt 1), 207–218. https://doi.org/10.1016/j.envpol.2017.07.105.

Calliari, E., Staccione, A., Mysiak, J., 2019. An assessment framework for climate-proof nature-based solutions. Sci. Total Environ. 656 (15 March 2019), 691–700. https://doi.org/10.1016/j.scitotenv.2018.11.341.

Carrus, G., Scopelliti, M., Lafortezza, R., Colangelo, G., Ferrini, F., Salbitano, F., Agrimi, M., Portoghesi, L., Semenzato, P., Sanesi, G., 2015. Go greener, feel better? The positive effects of biodiversity on the well-being of individuals visiting urban and peri-urban green areas. Landsc. Urban Plan. 134, 221–228. https://doi.org/10.1016/j.landurbplan.2014.10.022.

Cohen-Shacham, E., Walters, G., Janzen, C., Maginnis, S., 2016. Nature-Based Solutions to Address Global Societal Challenges. IUCN, Gland, Switzerland. https://doi.org/10.2305/IUCN.CH.2016.13.en xiii + 97pp.

Costanza, R., d'Arge, R., de Groot, R., Farber, S., Grasso, M., Hannon, B., Limburg, K., Naeem, S., O'Neill, R.V., Paruelo, J., Raskin, R.G., Sutton, P., van den Belt, M., 1997. The value of the world's ecosystem services and natural capital. Nature 387, 253–260. https://doi.org/10.1038/387253a0.

Currie, B.A., Bass, B., 2008. Estimates of air pollution mitigation with green plants and green roofs using the UFORE model. Urban Ecosyst. 11, 409–422. https://doi.org/10.1007/s11252-008-0054-y.

Davila, A.F., Rey, D., Mohamed, K., Rubio, B., Guerra, A.P., 2006. Mapping the sources of urban dust in a coastal environment by measuring magnetic parameters of Platanus hispanica leaves. Environ. Sci. Technol. 40, 3922–3928.

Dzierżanowski, K., Popek, R., Gawrońska, H., Sæbø, H., Gawroński, S.W., 2011. Deposition of particulate matter of different size fractions on leaf surfaces and in waxes of urban Forest species. Int. J. Phytoremed. 13 (10), 1037–1046. https://doi.org/10.1080/15226514.2011.552929.

Ebi, K.L., Vanos, J., Baldwin, J.W., Bell, J.E., Hondula, D.M., Errett, N.A., Hayes, K., Reid, C.E., Saha, S., Spector, J., Berry, P., 2021. Extreme weather and climate change: population health and health system implications. Annu. Rev. Public Health 42 (1), 293–315. https://doi.org/10.1146/annurev-publhealth-012420-105026.

Escobedo, F.J., Giannico, V., Jim, C.Y., Sanesi, G., Lafortezza, R., 2019. Urban forests, ecosystem services, green infrastructure and nature-based solutions: Nexus or evolving metaphors? Urban For. Urban Green. 37, 3–12. https://doi.org/10.1016/j.ufug.2018.02.011.

European Commission, 2015. Nature-based solutions & re-naturing cities. In: Final report of the horizon 2020 28 expert group on 'Nature-Based solutions and Re-Naturing cities'. https://doi.org/10.2777/765301.

European Environment Agency (EEA), 2016. Air Quality in Europe — 2016 Report. Publications Office of the European Union, Luxembourg. ISBN 978–92–9213-847-9.

Faivre, N., Fritz, M., Freitas, T., de Boissezon, B., Vandewoestijne, S., 2017. Nature-based solutions in the EU: innovating with nature to address social, economic and environmental challenges. Environ. Res. 159, 509–518. https://doi.org/10.1016/j.envres.2017.08.032.

Farrugia, S., Hudson, M.D., McCulloch, L., 2015. An evaluation of flood control and urban cooling ecosystem services delivered by urban green infrastructure. Int. J. Biodiv. Sci. Ecosyst. Serv. Manag. 9 (2), 136–145. https://doi.org/10.1080/21513732.2013.782342.

Griffith, D.W., Fraser, P.J., Galbally, I.E., 2021. Climate change: atmospheric facts and figures. Chem. Aust. (Jun-Aug 2021), 18–22.

Guidolotti, G., Salviato, M., Calfapietra, C., 2016. Comparing estimates of EMEP MSC-W and UFORE models in air pollutant reduction by urban trees. Environ. Sci. Pollut. Res. Int. 23 (19), 19541–19550. https://doi.org/10.1007/s11356-016-7135-x. Epub Jul 8. 27392620.

He, C., Qiu, K., Pott, R., 2020. Reduction of urban traffic–related particulate matter—leaf trait matters. Environ. Sci. Pollut. Res. 27, 5825–5844. https://doi.org/10.1007/s11356-019-07160-0.

Hirabayashi, S., Kroll, C.N., Nowak, D.J., 2012. i-Tree Eco Dry Deposition Model Descriptions.

Hui, K., Yuan, Y., Xi, B., Tan, W., 2023. A review of the factors affecting the emission of the ozone chemical precursors VOCs and NOx from the soil. Environ. Int., 107799 https://doi.org/10.1016/j.envint.2023.107799.

i-Tree Eco v.6.0, 2023. User Manual. https://www.itreetools.org/support/resources-overview/i-tree-manuals-workbooks.

Jafari, M., Knappe, D., Rehkop, N., Runte, J., Morgenstern, R., Störzner, A., Pölling, B., 2021. Dortmund living lab implementation plan. Deliverable No. 3.2, proGIreg. Horizon 2020 Grant Agreement No 776528, European Commission. Accessed April 03, 2021. https://progireg.eu/resources/planning-implementing-nbs/. Horizon 2020 Grant Agreement No 776528, European Commission. Accessed April 03, 2021.

Janhall, S., 2015. Review on urban vegetation and particle air pollution: deposition and dispersion. Atmos. Environ. 105, 130–137. https://doi.org/10.1016/j.atmosenv.2015.01.052.

Kabisch, N., Korn, H., Stadler, J., Bonn, A., 2017. Nature-Based Solutions to Climate Change Adaptation in Urban Areas - Linkages between Science, Policy and Practice. Springer, Cham. https://doi.org/10.1007/978-3-319-56091-5_1.

Lamb, W.F., Wiedmann, T., Pongratz, J., Andrew, R., Crippa, M., Olivier, J.G., Wiedenhofer, D., Mattioli, G., Al Khourdajie, A., House, J., Pachauri, S., 2021. A review of trends and drivers of greenhouse gas emissions by sector from 1990 to 2018. Environ. Res. Lett. 16 (7), 073005 https://doi.org/10.1088/1748-9326/abee4e.

Martin, N.A., Chappelka, A.H., Loewenstein, E.F., Keever, G.J., 2012. Comparison of carbon storage, carbon sequestration, and air pollution removal by protected and maintained urban forests in Alabama, USA. Int. J. Biodiv. Sci. Ecosyst. Serv. Manag. 8 (3), 265–272. https://doi.org/10.1080/21513732.2012.712550.

Massimi, L., Conti, M.E., Mele, G., Ristorini, M., Astolfi, M.L., Canepari, S., 2019. Lichen transplants as indicators of atmospheric element concentrations: a high spatial resolution comparison with PM10 samples in a polluted area (Central Italy). Ecol. Indic. 101, 759–769. https://doi.org/10.1016/j.ecolind.2018.12.051.

Massimi, L., Ristorini, M., Astolfi, M.L., Perrino, C., Canepari, S., 2020. High resolution spatial mapping of element concentrations in PM10: a powerful tool for localization of emission sources. Atmos. Res. 244, 105060 https://doi.org/10.1016/j.atmosres.2020.105060.

Merkus, H.G., 2009. Particle size measurements. In: Springer, S. (Ed.), Particle Technology.

Mikhaylov, A., Moiseev, N., Aleshin, K., Burkhardt, T., 2020. Global climate change and greenhouse effect. Entrepr. Sustain. Issues 7 (4), 2897. https://doi.org/10.9770/jesi.2020.7.4(21).

Millennium Ecosystem Assessment (Program), 2005. Ecosystems and Human Well-Being. Island Press, Washington, D.C.

Myeong, S., Nowak, D.J., Duggin, M.J., 2006. A temporal analysis of urban forest carbon storage using remote sensing. Remote Sens. Environ. 101, 277–282. https://doi.org/10.1016/j.rse.2005.12.001.

Nečas, D., Klapetek, P., 2012. Gwyddion: an open-source software for SPM data analysis. Open Phys. 10, 181–188. https://doi.org/10.2478/s11534-011-0096-2.

Nicese, F.P., Colangelo, G., Comolli, R., Azzini, L., Lucchetti, S., Marziliano, P.A., Sanesi, G., 2021. Estimating CO2 balance through the Life Cycle Assessment prism: A case – Study in an urban park. In: Urban Forestry & Urban Greening, 57, p. 126869. ISSN 1618-8667. https://doi.org/10.1016/j.ufug.2020.126869. ISSN 1618-8667.

Nowak, D.J., 1994. Atmospheric carbon dioxide reduction by Chicago's urban forest. In: McPherson, E.G., Nowak, D.J. (Eds.), Chicago's Urban Forest Ecosystem: Results of the Chicago Urban Forest Climate Project, 1994. US Department of Agriculture, Forest Service, Northeastern Forest Experiment Station, Radnor, PA, USA, pp. 83–94.

Nowak, D.J., Crane, D.E., 2002. Carbon storage and sequestration by urban trees in the USA. Environ. Pollut. 116 (3), 381–389. PII: S0269–7491(01)00214-7.

Nowak, D.J., Stevens, J.C., Sisinni, S.M., Luley, C.J., 2002. Effects of urban tree management and species selection on atmospheric carbon dioxide. J. Arboric. 28 (3), 113–122.

Nowak, D.J., Crane, D.E., Stevens, J.C., 2006. Air pollution removal by urban trees and shrubs in the United States. Urban For. Urban Green. 4, 115–123. https://doi.org/10.1016/j.ufug.2006.01.007.

Nowak, D.J., Hirabayashi, S., Bodine, A., Hoehn, R., 2013. Modeled PM2.5 removal by trees in ten US cities and associated health effects. Environ. Pollut. 178, 395–402.

Ordóñez, C., Grant, A., Millward, A., Steenberg, J., Sabetski, V., 2019. Developing performance indicators for nature-based solution projects in urban areas: the case of trees in revitalized commercial spaces. Cities Environ. (CATE) 12 (1).

Ottele, M., van Bohemen, H.D., Fraaij, A.L.A., 2010. Quantifying the deposition of particulate matter on climber vegetation on living walls. Ecol. Eng. 36, 154–162. https://doi.org/10.1016/j.ecoleng.2009.02.007.

Pace, R., Biber, P., Pretzsch, H., Grote, R., 2018. Modeling ecosystem Services for Park Trees: sensitivity of i-tree eco simulations to light exposure and tree species classification. Forests 9, 89. https://doi.org/10.3390/f9020089.

Pace, R., Guidolotti, G., Baldacchini, G., Pallozzi, E., Grote, R., Nowak, D.J., Calfapietra, C., 2021. Comparing i-tree eco estimates of particulate matter deposition with leaf and canopy measurements in an urban Mediterranean holm oak Forest. Environ. Sci. Technol. 55, 6613–6622. https://doi.org/10.1021/acs.est.0c07679.

Panno, A., Carrusa, G., Lafortezza, R., Mariani, L., Sanesi, G., 2017. Nature-based solutions to promote human resilience and wellbeing in cities during increasingly hot summers. Environ. Res. 159, 249–256. https://doi.org/10.1016/j.envres.2017.08.016.

Przybysz, A., Nersisyan, G., Gawroński, S.W., 2019. Removal of particulate matter and trace elements from ambient air by urban greenery in the winter season. Environ. Sci. Pollut. Res. 26, 473–482. https://doi.org/10.1007/s11356-018-3628-0.

Rafael, S., Vicente, B., Rodrigues, V., Miranda, A.I., Borrego, C., Lopes, M., 2018. Impacts of green infrastructures on aerodynamic flow and air quality in Porto's urban area. Atmos. Environ. 190, 317–330. https://doi.org/10.1016/j.atmosenv.2018.07.044.

Riondato, E., Pilla, F., Basu, A.S., Basu, B., 2020. Investigating the effect of trees on urban quality in Dublin by combining air monitoring with i-tree eco model, sustainable cities and society, 61, 102356. ISSN 2210–6707. https://doi.org/10.1016/j.scs.2020.102356. ISSN 2210–6707.

Ristorini, M., Astolfi, M.L., Frezzini, M.A., Canepari, S., Massimi, L., 2020a. Evaluation of the efficiency of *Arundo donax* L. leaves as biomonitors for atmospheric element concentrations in an urban and industrial area of Central Italy. Atmosphere 11, 226. https://doi.org/10.3390/atmos11030226.

Ristorini, M., Baldacchini, C., Massimi, L., Sgrigna, G., Calfapietra, C., 2020b. Innovative characterization of particulate matter deposited on urban vegetation leaves through the application of a chemical fractionation procedure. Int. J. Environ. Res. Public Health 17, 5717. https://doi.org/10.3390/ijerph17165717.

Ruangpan, L., Vojinovic, Z., Di Sabatino, S., Leo, L.S., Capobianco, V., Oen, A.M.P., McClain, M.E., Lopez-Gunn, E., 2020. Nature-based solutions for hydro-meteorological risk reduction: a state-of-the-art review of the research area. Nat. Hazards Earth Syst. Sci. 20 (243–270), 49. https://doi.org/10.5194/nhess-20-243-2020.2020.

Sæbø, A., Popek, R., Nawrot, B., Hanslin, H.M., Gawronska, H., Gawronski, S.W., 2012. Plant species differences in particulate matter accumulation on leaf surfaces. Sci. Total Environ. 427–428, 347–354.

Schneider, C.A., Rasband, W.S., Eliceiri, K.W., 2012. NIH image to ImageJ: 25 years of image analysis. Nat. Methods 9, 671–675.

Seddon, N., Chausson, A., Berry, P., Girardin, C., Smith, A., Turner, B., 2020. Understanding the value and limits of nature-based solutions to climate change and other global challenges. Philosoph. Trans. Royal Soc. B: Biol. Sci. 375, 20190120. https://doi.org/10.1098/rstb.2019.0120.

Sgrigna, G., Baldacchini, C., Dreveck, S., Cheng, Z., Calfapietra, C., 2020. Relationships between air particulate matter capture efficiency and leaf traits in twelve tree species from an Italian urban-industrial environment. Sci. Total Environ. 718, 137310 https://doi.org/10.1016/j.scitotenv.2020.137310.

Shi, J., Zhang, G., An, H., Yin, W., Xia, X., 2008. Quantifying the particulate matter accumulation on leaf surfaces of urban plants in Beijing, China. Atmosph. Poll. Res. 8, 836–842. https://doi.org/10.1016/j.apr.2017.01.011.

Singh, K., Tripathi, D., 2021. Particulate matter and human health. In: Environmental Health. IntechOpen Limited, United Nation, pp. 33–48. Available online at. https://www.intechopen.com/chapters/79308. https://doi.org/10.5772/intechopen.100550.

Song, Y., Kirkwood, N., Maksimović, C., Zheng, X., O'Connor, D., Jin, Y., Hou, D., 2019. Nature based solutions for contaminated land remediation and brownfield redevelopment in cities: a review. Sci. Total Environ. 663, 568–579. https://doi.org/10.1016/j.scitotenv.2019.01.347.

Tan, X., Liu, Y., Dong, H., Xiao, Y., Zhao, Z., 2022. The health consequences of greenhouse gas emissions: a potential pathway. Environ. Geochem. Health 1–20. https://doi.org/10.1007/s10653-021-01142-3.

Taylor, J.R., 1982. An Introduction to Error Analysis, 2nd ed. University Science Book, Sausalito, California (USA).

Tomašević, M., Vukmirović, Z., Rajšić, S., Tasić, M., Stevanović, B., 2005. Characterization of trace metal particles deposited on some deciduous tree leaves in an urban area. Chemosphere 61 (6), 753–760. ISSN 0045–6535. https://doi.org/10.1016/j.chemosphere.2005.03.077. ISSN 0045–6535.

Tuckett, R., 2021. Greenhouse gases and the emerging climate emergency. In: Climate Change, 19-45. Elsevier. https://doi.org/10.1016/B978-0-12-821575-3.00002-5.

Wang, H., Shi, H., Wang, Y., 2015. Effects of weather, time, and pollution level on the amount of particulate matter deposited on leaves of Ligustrum lucidum. Hindawi Publish. Corp. Sci. World J. 8. https://doi.org/10.1155/2015/935942. Article ID 935942.

Weerakkody, U., Dover, J.W., Mitchell, P., Reiling, K., 2017. Particulate matter pollution capture by leaves of seventeen living wall species with special reference to rail-traffic at a metropolitan station. Urban For. Urban Green. 27, 173–186. ISSN 1618–8667. https://doi.org/10.1016/j.ufug.2017.07.005. ISSN 1618–8667.

Xu, X., Zhang, Z., Bao, L., Mo, L., Yu, X., Fan, D., Lun, X., 2017. Influence of rainfall duration and intensity on particulate matter removal from plant leaves. Sci. Total Environ. 609, 11–16. ISSN 0048–9697. https://doi.org/10.1016/j.scitotenv.2017.07.141. ISSN 0048–9697.

Zang, C., Hartl-Meier, C., Dittmar, C., Rothe, A., Menzel, A., 2014. Patterns of drought tolerance in major European temperate forest trees: climatic drivers and levels of variability. Glob. Chang. Biol. 20, 3767–3779. https://doi.org/10.1111/gcb.12637.